

Development of optimization algorithms for electromagnetic characterization in free space

José Cidrás Estévez*, David Ramos Somolinos*, Borja Plaza Gallardo*, David Poyatos Martínez*

*National Institute for Aerospace Technology, INTA, Torrejon de Ardoz, Madrid, Spain, poyatosmd@inta.es

Abstract—In recent years, in the aerospace industry, there has been a trend based on replacing the classic metallic materials with new advanced materials such as carbon fiber composites (CFC), fiberglass, etc. Due to this, the electromagnetic (EM) characterization of these new materials is essential to maintain safety and EM compatibility. This article will focus on the free space measurement technique, from which a series of optimization algorithms have been developed, allowing the extraction of permittivity and permeability of materials in a frequency range up to 40 GHz using the Time-Domain Gating from a Vector Network Analyzer (VNA).

Index Terms—optimization algorithms, free-space method, scattering parameters, time-domain gating, material characterization, non-destructive testing, permeability, permittivity.

I. INTRODUCTION

During the last decade, new generation composite materials have gained greater importance as design materials in many industries, mainly due to their low weight and excellent structural performance. Among them, 3D printing stands out due to its ease of design and low cost, and composite materials due to their low weight while maintaining good rigidity and structural resistance. This is why they are widely used in both the aerospace and automotive industries [1].

The need for electromagnetic (EM) characterization of this type of materials can be demonstrated in a couple of examples. Compared to the classic metal surfaces used in aircraft [2], carbon fiber composites have less effective shielding, so studying this characteristic is essential to preserve the proper functioning of electronic devices located within these platforms. Other than that, the EM characteristics of the 3D printed materials differ from the initial raw materials, as a result of the phase change from liquid to solid state in the manufacturing process. In addition, the fill density in the final samples could modify properties such as their permittivity or the loss tangent [3].

Therefore, the importance of EM characterization of these new materials and the need to investigate modern and more flexible characterization methods is clear.

Currently there are different methods of electromagnetic characterization of materials at microwave frequencies, including transmission lines, resonant cavities or impedance analysis [4]. The use of free space measurement methods has become the most common method for characterization in the microwave region due to its ease of use and its reasonable accuracy [5]. However, free space measurement



Fig. 1. Free space measurement bench with high precision polyrod antennas.

methods have certain disadvantages, for example problems at certain resonant frequencies due to the sample thickness or the low precision in the calculation of the imaginary part of the permittivity in dielectric materials with low losses.

This article is focused on the development of permittivity and permeability extraction algorithms from free space measurement technique in the Computational and Applied Electromagnetism Laboratory (CAEM-Lab) of the National Institute of Aerospace Technology (INTA), using the measurement system known as POLYBENCH (see figure 1).

The content of this article is structured as follows: section II describes the method for obtaining the reflection and transmission coefficients from measurements in free space and their theoretical calculation; section III presents the types of algorithms used to obtain the permittivity and permeability of the measured materials; section IV compares the results obtained with each of the algorithms described in III and section V draws the conclusions.

II. REFLECTION AND TRANSMISSION PARAMETERS

The interaction of the material under test (MUT) with the EM field is defined by the dielectric permittivity ϵ (F/m) and the magnetic permeability μ (H/m) [6]. Both parameters can be written in a complex and dimensionless form as follows [4]:

$$\epsilon = \epsilon_0 \epsilon_r = \epsilon_0 (\epsilon_r' - i\epsilon_r'') \quad (1)$$

$$\mu = \mu_0 \mu_r = \mu_0 (\mu_r' - i\mu_r'') \quad (2)$$

Where ϵ_0 and μ_0 are the permittivity and permeability of vacuum, respectively. These last two parameters can be related to the reflection and transmission coefficients and the developed optimization algorithms are based on this idea.

A. Measurement of reflection and transmission parameters

The test is based on obtaining the values of the reflection and transmission coefficient of a material from the scattering (S) parameters. Obtaining the S-parameters in the test bench is done by means of a Vector Network Analyzer (VNA). In the case of study, since there are two antennas facing each other, it will be interesting to obtain the values of the parameters S_{11} (emitting the signal through port 1 and receiving it in the same port) and S_{21} (transmitting the electromagnetic signal through port 1 and receiving it in port 2), see figure 2.

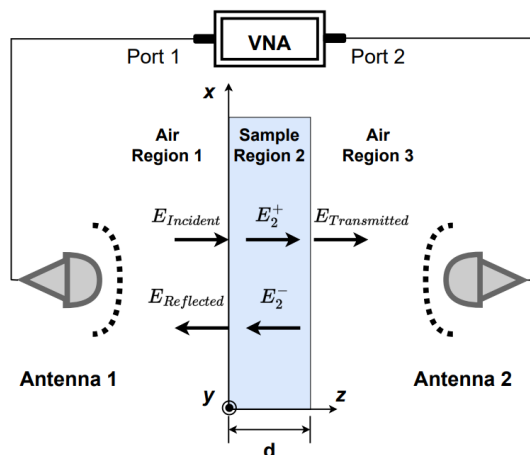


Fig. 2. Representation of the transmission and reflection free space technique. The sample is placed between two antennas, which are connected to the ports of the VNA.

A total of three measurements are made for each material to be tested and for each of the S-parameters. The MUT is measured fixed as it appears in the figure 1. Then, in a second measurement, the S-parameters of free space (air) are obtained, and finally, the third measurement corresponds to a metal plate. Once the parameters S_{11} and S_{21} are known, the reflection and transmission values can be extracted from them, see [7].

B. Theoretical equation of the reflection and transmission coefficients

The equation that links permittivity and permeability of the MUT with the measured reflection and transmission coefficients is based on the interaction of a wave that propagates in the air and impinges perpendicularly on a material other than air and with a certain thickness.

This propagation can be divided into three parts, as shown in figure 2. First of all, in the area to the left of the material there will be an incident and reflected wave (produced by the first reflection in the discontinuity of the material whose direction will be assumed to be $-z$). In the second part, inside the material, there will be propagation in both directions due to the multiple reflections of the wave inside the material and in the third part, the right side of the material, there will be the transmitted wave (produced by the first transmission and by the propagation of the wave in the $+z$ direction inside the material).

Thus, the total reflection and transmission of the wave can be calculated taking into account the theory of normal wave propagation in these three propagation zones. In this way, following the formulation of [8] and [9] the reflection (Γ) and transmission (T) coefficients can be expressed according to the complex permittivity and permeability as follows:

$$T_{total} = \frac{4\sqrt{\frac{\mu_2}{\epsilon_2}} e^{-j\omega d\sqrt{\epsilon_0\mu_0\epsilon_2\mu_2}}}{\left(1 + \sqrt{\frac{\mu_2}{\epsilon_2}}\right)^2 - e^{-2j\omega d\sqrt{\epsilon_0\mu_0\epsilon_2\mu_2}} \left(1 - \sqrt{\frac{\mu_2}{\epsilon_2}}\right)^2} \quad (3)$$

$$\Gamma_{total} = \frac{\left(\frac{\mu_2}{\epsilon_2} - 1\right) \left(1 - e^{-2j\omega d\sqrt{\epsilon_0\mu_0\epsilon_2\mu_2}}\right)}{\left(1 + \sqrt{\frac{\mu_2}{\epsilon_2}}\right)^2 - e^{-2j\omega d\sqrt{\epsilon_0\mu_0\epsilon_2\mu_2}} \left(1 - \sqrt{\frac{\mu_2}{\epsilon_2}}\right)^2} \quad (4)$$

Where ϵ_2 and μ_2 are respectively the permittivity and permeability of the MUT.

III. OPTIMIZATION ALGORITHMS EMPLOYED

This section shows the different algorithms used to obtain the complex permittivity and permeability values.

A. Iterative methods

Within this section, various iterative algorithms have been used, based on the minimization of an error function, in which the measured reflection and transmission values and the theoretical values of equations 3 and 4 are subtracted.

On the one hand, some algorithms that are already implemented in Matlab were used and, on the other hand, our own algorithms have been developed.

1. Algorithms already implemented in MATLAB:

- **FMINCON**[10]: Optimization solver to find the minimum of a multivariable function, with the possibility of imposing a confidence region (limiting the solutions). Two types of algorithms have been used, SQP= "Sequential Quadratic

Programming” and IP= ”interior-point”, similar to Newton-Raphson but using the commented trust region.

- **FSOLVE**[10]: Nonlinear systems solver. Where the LMA= “Levenberg–Marquardt algorithm” is used, which interpolates between Gauss-Newton algorithms (GNA) and the descending gradient method.

2. Own Algorithms:

- **Newton-Raphson**: A formulation is followed in which the real and imaginary parts are separated, so that four unknowns appear in the problem (real and imaginary parts of permittivity and permeability). Its implementation follows the following equation:

$$X^{new} = X^{old} \pm J^{-1}f \quad (5)$$

Where X corresponds to a vector with the four searched parameters, J is the Jacobian of the system of equations 3 and 4, and f is the error function mentioned above.

- **Gauss-Seidel**: In this case, this method is applied to the complex field. From equations 3 and 4 new variables are named: $X = \sqrt{\mu_2 \varepsilon_2}$, $Y = \sqrt{\mu_2 / \varepsilon_2}$, $K = dw \sqrt{\varepsilon_0 \mu_0}$ and $Z = e^{-iKY}$. The new variable Z is solved in the two equations and the solution is obtained through an iterative process. Once Z is obtained, in order to obtain the parameter Y , it is necessary to apply the natural logarithm to Z , which is a complex number, so infinite solutions are obtained. The choice of the correct solution can be made by applying certain restrictions in the code, taking into account the thickness of the material, the type of material or the frequency range used.

B. Heuristic method

In this case, the Particle Swarm Optimization (PSO) method, described in [11], is used. It is a genetic algorithm-style optimizer that is based on the application of a model present in nature to solve engineering problems. This method has been implemented using Matlab, and its search for complex permittivity and permeability parameters is based on the minimization of an error function similar to the one discussed in section III-A. This error function has been implemented in different ways in order to study which is the most appropriate searching for the solution. In this way, error functions have been implemented based on pure complex numbers, on module and phase or taking into account arithmetic means or variances.

IV. RESULTS OBTAINED

This section will analyze the measurements made to obtain the reflection and transmission parameters and the results obtained of permittivity and permeability values extracted with each implemented algorithm.

In order to validate all the algorithms mentioned, Teflon will be used, as it is one of the most used materials as a reference for electromagnetic characterization purposes. It has a real permittivity value of 2.1, stable in a wide frequency range [8], which will serve to validate the algorithms used.

In addition, for algorithm validation, the results of the real part of the permittivity of other materials will be compared.

These materials are reference materials with known EM characteristics commercialized as Eccostock Hick from Laird Technologies Inc. [12]. In this case, the frequency range is extended from 3 to 40 GHz and Teflon results will be displayed again, now within a higher frequency range.

Once the algorithms have been validated, measurements of two types of composite materials will be shown in section IV-C.

A. Validation of the transmission and reflection equations

Taking into account the validation process of the reflection and transmission measurements, a comparative graph between the values that have been obtained for Teflon and the expected theoretical values of this material will be shown. All of them in the frequency range from 6 to 13 GHz.

To obtain the theoretical reflection and transmission coefficients, the permittivity reference value of $\varepsilon = 2.1 - 0.002j$ [13] has been used and $\mu = 1$ as permeability, for being a non-magnetic material. Knowing also that the Teflon sample has a thickness of 1 cm, these theoretical values have been calculated from equations 3 and 4.

As can be seen in figures 3 and 4, very similar values are obtained, although it can be seen, considering the error between the measurements and the theoretical values, that there is some variation in the region between 10 and 11 GHz, where most of these errors are congregated. This occurs due to the existence in that area of a resonance frequency, which implies a loss of precision when reflection signal level decreases diminishing the measured signal to noise ratio.

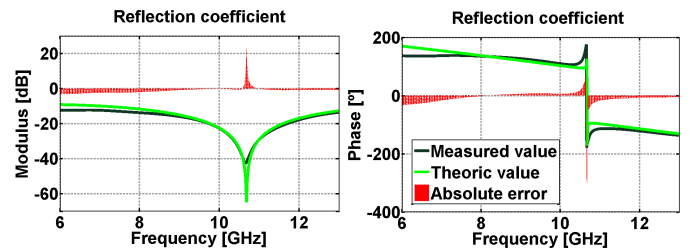


Fig. 3. Comparative graph of the measured and theoretical reflection modulus (dB) and phase (degrees) of a Teflon sample with a thickness of $d=1$ cm.

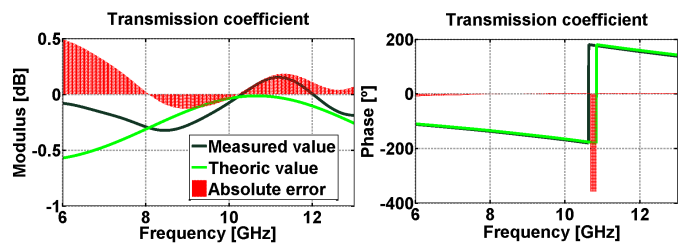


Fig. 4. Comparative graph of the measured and theoretical transmission modulus (dB) and phase (degrees) of a Teflon sample with a thickness of $d=1$ cm.

B. Algorithms validation

In order to validate the algorithms, the results obtained between 6 and 10 GHz are presented below. In this way, the resonant area is avoided (see figures 3 and 4) where measurement precision is deteriorated and thus validation is not affected.

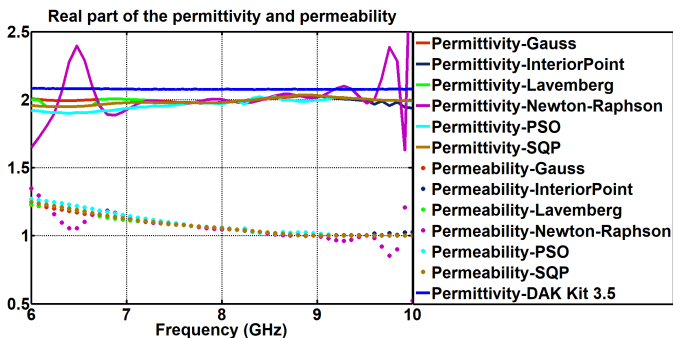


Fig. 5. Real part of the Teflon relative permeability and permittivity using different algorithms.

Apart from the free space method, the Open-Ended Coaxial Probe (OECF) method [14] has been used, so that the values obtained with Teflon with this method and the values obtained with each of the algorithms in free space can be compared (see figure 5). For the OECF technique, the DAK-3.5 kit, from SPEAG [15] has been used, which includes commercial software for automatic estimation of complex permittivity. This method has been validated in other studies made [14].

In this way, the permittivity and permeability values obtained with each of the exposed proposed are shown in figure 5 and table I, comparing also these results with the Teflon reference value. The presented values in table I have been obtained by averaging the permittivity and permeability values within the frequency range from 6 to 10 GHz. At the same time, a comparison is also made between the calculation times for each algorithm.

TABLE I
COMPARISON BETWEEN PRESENTED METHODS

Method	Frequencies [6-9 GHz]		Running time [s]
	ϵ	μ	
Reference value	2.1-0.002j	1	-
DAK Kit	2.0797-0.0007j	-	-
PSO	1.9674-0.0045j	1.086-0.0046j	63.2
Gauss	1.9942-0.0079j	1.1017-0.004j	5.1
Lavemberg	1.9935-0.0098j	1.0724-0.006j	4.3
Interior Point	1.9829-0.0039j	1.0769-0.0044j	9.6
SQP	1.9877-0.0026j	1.0746-0.005j	4.5
Newton-Raphson	2.0427-0.0024j	1.0531-0.0013	4.7

Moreover, three materials called Eccostock Hick K3, K5 and K7 have been measured, and the results are shown in figure 6. These three materials present values of the real part of the permittivity equal to 3, 5 and 7 respectively. Teflon will also be shown in this new frequency range.

In this case, only the values obtained from the PSO algorithm are shown, since it has been seen that with this

algorithm, more stable values are obtained in a wide range of frequencies; being able to avoid errors in the estimation of the permittivity on the resonant areas commented in previous section.

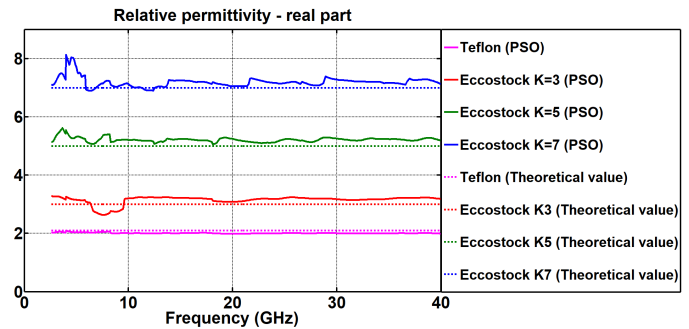


Fig. 6. Real part of the Teflon and Eccostock Hick relative permittivity using PSO algorithm.

As can be seen, adequate values are obtained for the real part of the permittivity of all of these materials after comparing the results obtained with their theoretical values.

C. Other measurements

Finally, the results of two types of composite materials will be shown in this section. Both, a sample of quartz fiber composite material and a polyethylene sample. The stacking sequence of each of the samples and their properties are found in Table II. Note that the chosen materials are non-magnetic ($\mu_r = 1$) and do not conduct electricity; therefore, only the permittivity will be analyzed, and its expected imaginary part will be very low.

TABLE II
PREPEG OF QUARTZ AND POLYETHYLENE FIBERS, LAMINATES PROPERTIES.

Material	Stacking Sequence	Resin	Theoretical permittivity real part
Polyethylene	[(0/90)] ₃₄	Epolam 2025	2.8
Quartz	[(0/90)] ₁₄	Epolam 2025	3.1

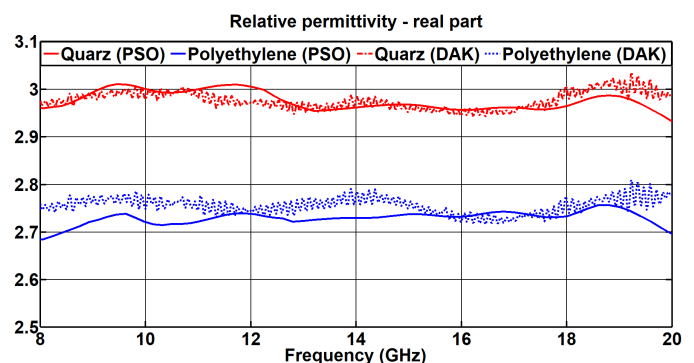


Fig. 7. Comparison, from 8 to 20 GHz, between the real part of the permittivity of quartz fiber (in red) and polyethylene (in blue), obtained with Free-space + PSO and OECF methods.

It is estimated that the value of the real part of the permittivity for these materials, based on the type of fiber and resin used, is 2.8 in the case of polyethylene fiber and 3.1 in the case of quartz fiber (see Table II) [16]. The results obtained from the measurements made are depicted in Figure 7, where both results obtained with the DAK Kit and with the PSO algorithm are similar to those found in the literature.

V. CONCLUSIONS

It has been possible to validate the different extraction algorithms using Teflon as a reference material, comparing the results obtained with theoretical values and with measurements extracted with another commercial measurement system, the DAK Kit.

Also, problems have been reported when determining the permittivity and permeability at frequencies where resonances occur in the material. This appears when the thickness of the sample coincides with half the wavelength, so this effect can be mitigated by measuring the same material with different thicknesses.

Finally, it can be concluded that Gauss and Newton-Raphson algorithms have a greater limitation of use, since they require an estimation of the expected permittivity and permeability (starting point) and no restrictions in the calculation can be imposed, that is, upper or lower limits for solutions. It may happen that they do not converge to a solution, as is the case between 10 and 11 GHz with Teflon. In the case of the rest of the studied algorithms, both those included in Matlab or PSO, they always reach solutions by being able to restrict the search space. In addition, as can be seen in the results obtained with the Eccostock materials and the composite materials (figures 6 and 7), by means of the PSO method it has been possible to avoid the error on the permittivity estimation in the resonant zones.

Regarding the execution time of each algorithm, it can be seen how the iterative type algorithms are faster than PSO. Said slowness in the PSO will depend to a greater extent on the size of the search space and the number of variations of this space throughout the algorithm. However, through PSO, the solution does not depend on a starting point as it happens with the rest of the algorithms, since its operation is not based on an iterative process of a single solution. The PSO looks for a set of possible solutions, which are updated in each iteration, so that the solution obtained will be the one that minimizes the error.

ACKNOWLEDGMENT

This work has been partially funded by the Ministry of Science and Innovation (MICINN) within the framework of the eSAFE-UAV project (PID2019-106120RB-C32).

REFERENCES

[1] A. Baker, D. SE, and D. Kelly, *Composite Materials for Aircraft Structures*, 06 AIAA Education Series, 2004.

[2] M. R. Cabello, S. Fernández, M. Pous, E. Pascual-Gil, L. D. Angulo, P. López, P. J. Riu, G. G. Gutierrez, D. Mateos, D. Poyatos, M. Fernandez, J. Alvarez, M. F. Pantoja, M. Añón, F. Silva, A. R. Bretones, R. Trallero, L. Nuño, D. Escot, R. G. Martín, and S. G. Garcia, "Siva uav: A case study for the emc analysis of composite air vehicles," *IEEE Transactions on Electromagnetic Compatibility*, vol. 59, no. 4, pp. 1103–1113, Aug 2017.

[3] D. P. Martínez, D. R. Somolinos, and B. P. Gallardo, "Electromagnetic characterization of materials through high accuracy free space measurements," *15th European Conference on Antennas and Propagation (EuCAP)*, March 2021.

[4] M. T. Jilani, "A brief review of measuring techniques for characterization of dielectric materials," *International Journal of Information Technology and Electrical Engineering*, 12 2012.

[5] J. W. Schultz, *Focused Beam Methods, Measuring Microwave Materials In Free Space*. Amazon Distribution, 2012.

[6] M. Barmatz, D. Steinfeld, D. Winterhalter, D. Rickman, R. Gustafson, D. Butts, and M. Weinstein, "Microwave permittivity and permeability measurements on lunar simulants," *Lunar and Planetary Science Conference*, 2012.

[7] D. R. Somolinos, J. C. Estévez, B. P. Gallardo, C. Moravec, A. de la Torre, M. R. K. Frövel, and D. P. Martínez, "Novel electromagnetic characterization methods for new materials and structures in aerospace platforms," *MDPI, materials*, no. 15, July 2022.

[8] C. A. Balanis, *ADVANCED ENGINEERING ELECTROMAGNETICS*. Jhon Wiley Sons, Inc., 1989.

[9] D. T. Paris and F. K. Hurd, *Basic Electromagnetic Theory*. McGraw-Hill, New York, 1969.

[10] "The Math Works, Inc." MATLAB, Computer software V.2012b. [Online]. Available: <https://www.mathworks.com/>.

[11] J. Kennedy and R. C. Eberhart, *Particle swarm optimization*, ser. Piscataway, NJ. Proc. IEEE Conf. Neural Networks IV, 1995.

[12] "Eccostock hik 500, high temperature tuned low loss dielectric stock," *Laird technologies, A DuPont Business*, vol. Product description, 2022. [Online]. Available: <https://www.laird.com/products/microwave-absorbers/low-loss-dielectrics/eccostock-hik-500>

[13] M. D. Belrhiti, S. Bri, A. Nakheli, and A. Mamouni, "Complex permittivity of low loss materials in the x band," *International Journal of Science and Advanced Technology*, vol. 1, no. 16, Aug. 2011.

[14] J. C. Estévez, B. P. Gallardo, D. R. Somolinos, N. S. Stepanyan, A. Cowley, and D. P. Martínez, "Electromagnetic characterization of lunar regolith simulants," *European Conference on Antennas and Propagation*, vol. Session M02: Satellite and aerospace antenna characterisation, Madrid Friday, 1 April, 2022.

[15] *DAK, Professional Handbook V2.0*. Schmid & Partner Engineering AG, May 5, 2015. [Online]. Available: <https://speag.swiss/>

[16] D. Kozakoff, *Analysis of Radome-Enclosed Antennas*. 2nd ed.; Artech House Inc.: Boston, London; ISBN 13: 978-1-59693-441-2., 2016.